



Simulation of a giant MSF recirculation plants

Adel K. El-Feky

Atomic Energy Authority, Inshas, Egypt

Tel. +20 1069767031; email: elfiqi02@hotmail.com

Received 2 December 2011; Accepted 18 July 2012

ABSTRACT

This study describes the mathematical model that used for the prediction of the performance of the multi-stage flash plant (MSF) systems under steady state conditions. The developed model based on the mass, heat, and energy balance. The governing equations describe the behavior of temperatures, brine, and product streams within the flashing stage. The losses, densities, enthalpies, and other properties are (accounted) for the model. This model consists of sets of algebraic equations. The proposed model was validated by another data from previous models and by an actual data from existing plants. This model focuses on the evaluation of flow rate and temperatures profile. This model can be used for small and large capacity plants that vary in the range of 5,000–77,760 m³/d. Through this study, both the specific heat transfer area and the weir load vary in the range of 175–300 m²/kg/s and 150–310 kg/s/m, respectively, also the stage width varies up to 25 m and the stage length varies in the range of 2–6 m.

Keywords: Modeling; Simulation; BR-MSF; Developing MSF design

1. Introduction

Most of the sea water desalination plants are of the multi-stage flash (MSF) type. They usually operate at top brine temperatures of 90–120°C. One of the main factors that affect the thermal efficiency of the plant is the difference in temperature from the brine heater to the end of the plant (flash range). Operating a plant at the higher temperature limits of 120°C tends to increase the efficiency, but it is also increases the potential for detrimental scale formation and accelerated corrosion rate. Through the accumulated experience obtained from the operation of the MSF plants around the world, the unit capacity increased to 50,000–70,000 m³/d.

For MSF desalination systems, steady state mathematical models were established. The models include

modeling and simulation of a multi-stage desalination plant [1] with 15 recovery stages and three rejection stages. The study based on both steady and dynamic simulations, and the study was performed using a FORTRAN program for steady state simulation and also through a SPEEDUP package. The plant under study is located at Umm AlNar, UAE. Its capacity is 6 mgd. The study is carried out under various operating conditions, and an operating analysis made for plant with sea water temperature constant at 35°C for summer conditions and 24°C for winter conditions.

There is another model [2] for steady state conditions for Al-Khobar2 to test the plant performance over extended ranges of TBT and cooling sea water temperatures.

This study is focused on modeling and simulation of the large-scale MSF design. The model describes the analysis of many parameters that affect on the design and operation performance of the plants, such as flow rates, temperatures, top brine temperature, plant productivity, and specific heat transfer area. There are many detailed steady state models for evaluating the thermodynamic losses and heat transfer coefficients [3]. Many models are established in the literature for calculating the performance ratio (PR), heat transfer area, and various stream flow rates [4,5].

2. MSF process

In the MSF process, sea water is heated in a vessel called brine heater. This is performed by condensing steam on a bank of tubes that carry sea water which pass through the vessel. This heated sea water then flows into another vessel, called a stage, where the ambient pressure is lower, causing the sea water to rapidly boil, with a portion flashing into steam. The sea water passes through around 20 stages each at a lower pressure.

Fig. 1 shows the process flow diagram of a brine recirculation MSF plant [10]. The main advance in MSF, over the earlier submerged tube multiple effect plants, is that evaporation takes place by flashing from a stream of brine flowing through the bottom of the stages, instead of direct contact boiling under stagnant conditions.

The latent heat that transfers from the brine to vapor causes the brine temperature to fall in each stage, approaching equilibrium with the saturated vapor conditions. After passing through the demisters to remove water droplets, the vapor is condensate on the surface of the heat exchanger tubes and the distillate product is collected.

Brine extracted from the lowest temperature stage is circulated through the tube bundles of the heat recovery stages and is heated by transfer of latent heat from the condensing vapor. A further temperature rise takes place in the brine heater to provide the temperature differential needed to promote flash evaporation. The lowest temperature stages, which are sea water cooled, act as a heat rejection section.

The distillate output of the MSF process is determined by the product of brine recirculation flow and the temperature difference between the brine heater outlet and the lowest stage temperature.

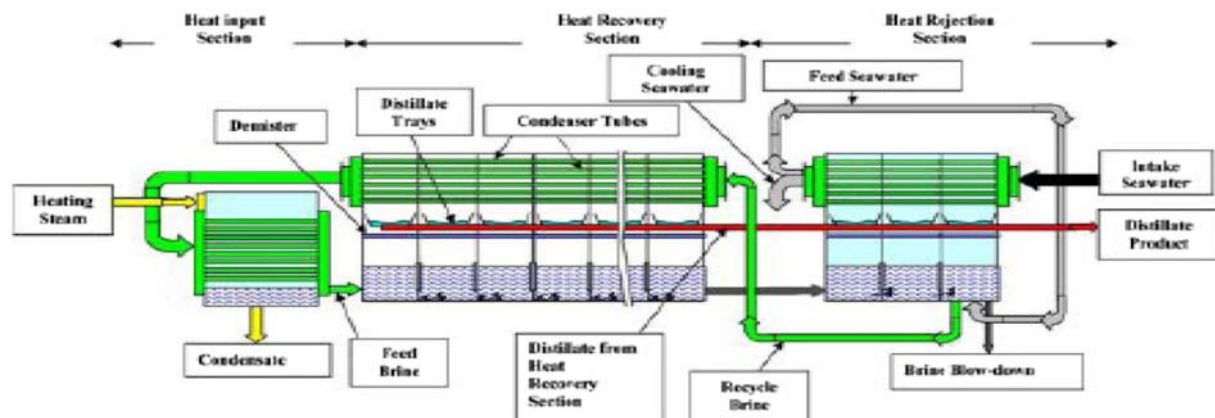
Distillate output from MSF does not depend directly on the heat transfer tube surface area or degree of fouling. However, both these factors and the number of stages determine the heat consumption of the process. Heat consumption is usually defined in terms of a PR, where the is defined as mass of distillate product per unit mass of steam consumed.

$$PR = \frac{\text{distillate output}}{\text{steam consumption}}$$
 the steam consumption is normally measured as saturated steam.

Typical values of PR are in the range of 7–10. An increase in the PR requires large heat transfer areas and usually a greater number of stages. The PR can be optimized by evaluating energy saving against the additional capital costs.

The MSF requires sea water for cooling the heat rejection section and ejector condensers, part of the cooling water flow being then introduced as feed make-up to the system.

While the basic technology of the latest, very large MSF plants is similar to the early units, there have been major developments in scale control techniques, heat transfer, and the use of corrosion-resistant materials. In addition, there have been improvements in



Source: H. El-Dessouky and H. Ettouy, "Study on water desalination technologies", prepared for ESCAWA in January 2001.

Fig. 1. Illustrates the process flow diagram of a brine recirculation MSF system.

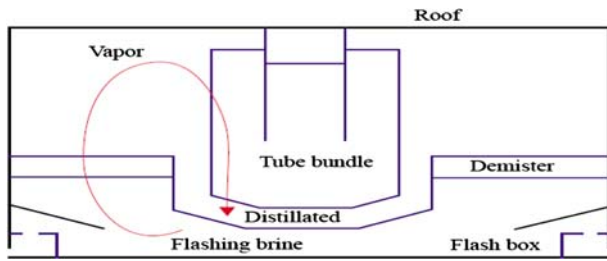


Fig. 2. Illustrates a cross-sectional view in a flashing stage.

the mechanical design of large structures and equipment such as the pumps that are now required.

Fig. 2 shows the schematic of the flashing stage, so the flashing stage consists of brine pool, submerged orifice, demister, tube bundle, air baffle, venting line, and product tray:

- The brine pool is the sump that the inlet brine flashes as its temperature is higher than the stage temperature.
- The submerged orifice is used for controlling the brine flow through the stage.
- The demister is designed for preventing any brine droplet from passing with the vapor to the tube bank.
- The vapor releases its latent heat to the tube bundle, heating the inside recirculating brine and the condensate vapor collected in the distillate tray.
- The air baffle is used to control the vapor flow through the vent line; 2.4% of the vapor in each stage is lost by the venting line, and about 92% of this lost vapor is recovered in the steam ejector condenser.
- The non-condensable gases should be extracted from each stage to prevent the insulating blanket around the tube bundle that can reduce the heat transfer coefficient; also, both oxygen and carbon dioxide in the non-condensable gases increase the corrosion rate for the stage materials.

Approximately, there are around nine pumps for the recirculation MSF units; these pumps are for, brine recirculation pump, intake sea water pump, feed sea water pump, rejected cooling sea water, distillate product pump, blow-down pump, steam condensate pump, ejector condensation pump and chemicals pump.

3. Mathematical model

The mathematical model of MSF desalination system was developed under these assumptions:

- It is a steady state operation model.
- Heat and mass losses to the surroundings and through the vacuum system are negligible.

- Vapor and liquid phase temperature in the evaporator are related to each other by the boiling point elevation (BPE).
- Thermodynamic losses in each flashing stage are BPE, non-equilibrium allowance NEA and demister losses.
- Perfect mixing of vapor and liquid stream.
- Condensate product in the brine heater is not subcooled.
- The specific heat at constant pressure, $C_p = 3.94 \text{ kJ/kg}^\circ\text{C}$.
- The product is salt-free.
- The latent heat of the vapor is temperature function.

The model equations are for the brine heater, the heat recovery section, and the heat rejection section. It is cleared that the balance of the heat recovery and heat rejection sections are similar [6,8].

The model for the MSF system was developed that relates the system design variables such as PR, TBT, recirculating flow M_{rec} Flow, and number of stages with the design and operating parameters such as temperature profile, flow profile, heat transfer coefficient and heat transfer area. Each stage is divided into four groups, Fig. 3 (flash chamber, vapor space, tube bundle, and product tray).

Applying the mass and energy balance equations for each of these groups, a system of equations is obtained.

Recovery section:

For a stage i of the recovery section, the stage salt balance is given by

$$M_b(i-1)X_b(i-1) = M_b(i)X_b(i) \quad (1)$$

The stage mass balance

$$M_b(i-1) + M_d(i-1) = M_b(i) + M_d(i) \quad (2)$$

The energy balance

$$M_b(i-1)h_b(i-1) = M_b(i)h_b(i) + [M_b(i-1) - M_b(i)]h_v(i) \quad (3)$$

The heat transfer equation for the condenser tubes

$$M_{\text{rec}} C_p (T_{f(i)} - T_{f(i+1)}) = U_{(i)} A_{(i)} \text{LMTD}_{(i)} \quad (4)$$

where

$$\text{LMTD}_{(i)} = \frac{T_{f(i)} - T_{f(i+1)}}{\ln \frac{T_d - T_{f(i+1)}}{T_d - T_{f(i)}}} \quad (5)$$

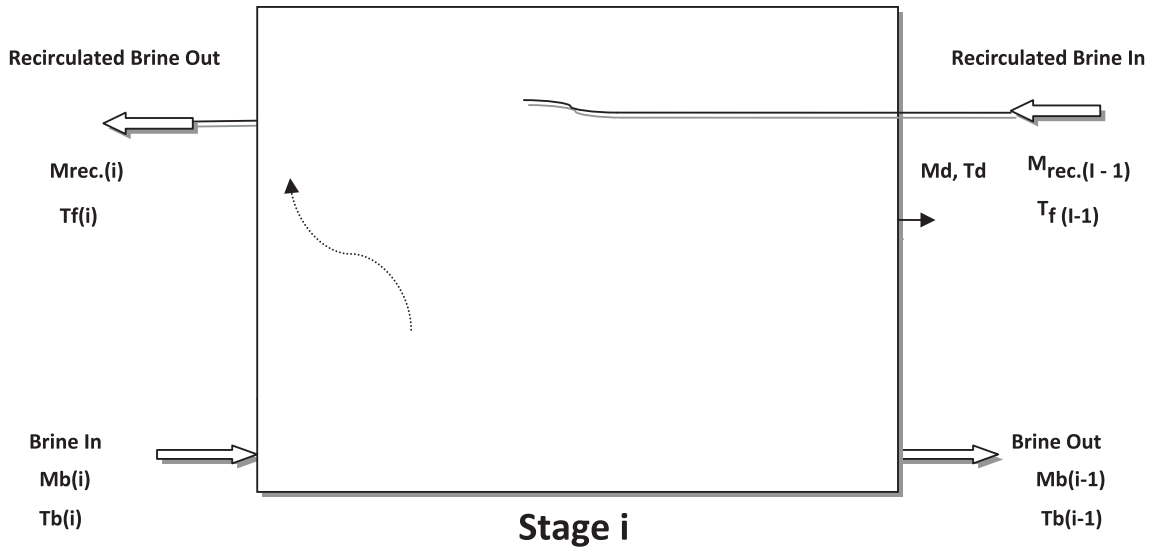


Fig. 3. Illustrates the four groups of each stage of the flashing chamber.

The heat transfer area for the recovery stage is given by

$$A_{(i)} = \frac{M_{rec} C_p \Delta T_c}{U_{(i)} LMTD_{(i)}} \quad (6)$$

For the product tray

$$M_{do} = M_{di} + M_{d(i)} \quad (7)$$

$$M_{do} h_o = M_{di} h_i + M_{d(i)} h_v \quad (8)$$

The product temperature

$$T_d = T_b - T_{losses} \quad (9)$$

where

$$T_{losses} = BPE + NEA + \Delta T_{demister} \quad (10)$$

Rejection section:

The total product is given by

$$M_D = M_{d(i)} + M_{d(j)} \quad (11)$$

The energy equation for the rejection stage is given by

$$(M_{cw} + M_f) C_p (T_{bd} - T_{sea}) = M_{d(r)} h_{d(r)} + M_{b(r)} h_{b(r)} - M_{rec} h_{bd} - M_D h_D - M_b h_{bd} \quad (12)$$

where

$$M_f = M_b + M_d \quad (13)$$

The heat transfer equation for the condenser is given as

$$A_j = \frac{(M_{cw} + M_f) C_p \Delta T_{cj}}{U_{(j)} LMTD_{(j)}} \quad (14)$$

Brine heater:

The energy balance equation for the brine heater

$$M_{rec} C_p \Delta T_{bh} = M_s h_{fg(s)} \quad (15)$$

The PR

$$PR = \frac{M_d}{M_s} \quad (16)$$

The brine temperature required through the brine heater

$$\Delta T_{bh} = \frac{M_d h_f g}{PR C_p M_{rec}} \quad (17)$$

The heat transfer equation for the brine heater

$$M_{rec} C_p \Delta T_{bh} = U_{bh} A_{bh} LMTD_{bh} \quad (18)$$

where

$$LMTD_{bh} = \frac{T_{BT} - T_1}{\ln \frac{T_s - T_1}{T_s - T_{BT}}} \quad (19)$$

The total heat transfer area of the MSF unit can be given as

$$A_{\text{total}} = A_i + A_j + A_{\text{bh}} \quad (20)$$

For the equation that governing the temperature losses, the heat transfer coefficient and the fouling factor can be observed in the index.

4. Solution method

The solution of the above equations starts with the defined design parameters, which are PR, distillate flow rate, number of stages, top brine temperature, steam temperature, intake sea water salinity.

So, the solution of these equations will result in feed, brine, distillate temperature profiles, the thermodynamic temperature losses, the heat transfer area of the recovery, rejection, brine heater, the cooling water flow rate, and the circulated brine flow rate.

All the physical properties, the thermodynamic losses governing equation, and the heat transfer coefficient will be illustrated in the Index.

5. Results

The developed model is used to investigate the effect of the design parameters on the unit performance. It can be also used to study the effect of operating conditions on the plant performance.

The analysis is performed for the design parameters shown in Table 1 for an actual plant in Oun Mossa, East of Egypt, on the Red Sea shore [1].

For the analysis, the data used are ranged as $M_d = 5,000\text{--}77,760 \text{ m}^3/\text{d}$, $TBT = 105\text{--}118^\circ\text{C}$.

Through the analysis of the MSF system, the calculation includes temperature profiles of the feed sea water, the brine temperature and the distillate temperature, specific flow rate of the entire stream, heat transfer areas for different sections.

Table 1
For actual data of Oun-Mossa

| Parameter | Value |
|---|--------|
| Distillate flow rate (m^3/d) | 5,000 |
| Intake sea water temperature ($^\circ\text{C}$) | 27 |
| Intake sea water salinity (ppm) | 45,000 |
| Brine salinity (ppm) | 70,000 |
| Top brine temperature ($^\circ\text{C}$) | 110 |
| Steam temperature for brine heater ($^\circ\text{C}$) | 117 |
| Number of stages | 20 |
| PR | 8 |

Figs. 4 and 5 illustrate a comparison between real and calculated temperature profiles of both feed and brine temperatures, as shown from the figures, there is a good agreement between the real and calculated temperatures profiles.

Fig. 6 illustrates the effect of the number of stages on the specific heat transfer area. As the number of stages increases, the specific heat transfer area requirement decreases. Thus, increasing the number of stages reduces the capital costs of the unit to a certain limit until the cost of manufacturing additional stages is greater than the saving in the heat transfer area.

As shown in Fig. 7, the specific heat transfer area decreases with increasing of the top brine temperature, this is because of the flash range increases, so temperature difference per each stage increase which increase the driving force. Also, the specific heat transfer area increases with the increase in the productivity of the plant as the steam consumption

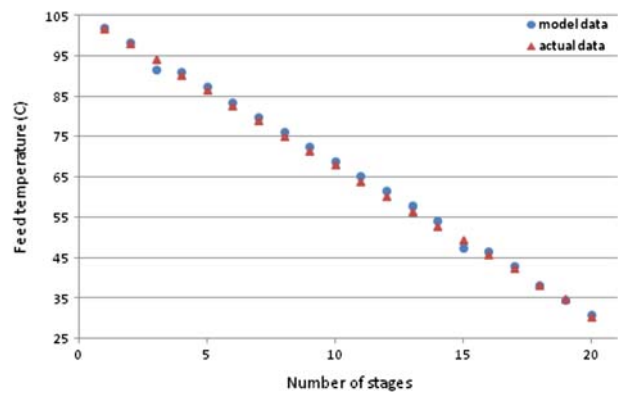


Fig. 4. Variation between actual feed temperature and model predicted one.

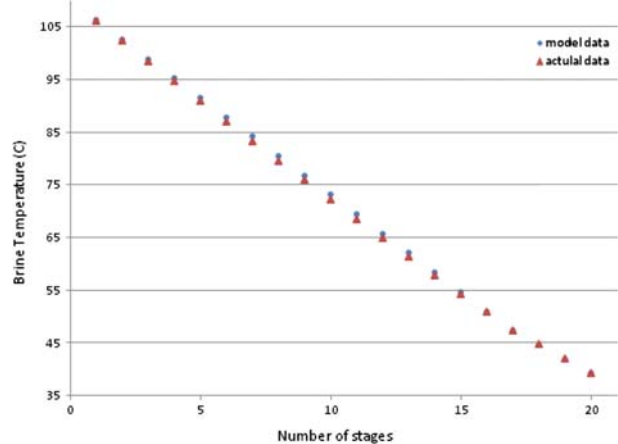


Fig. 5. Variation between actual brine temperature and predicted one.

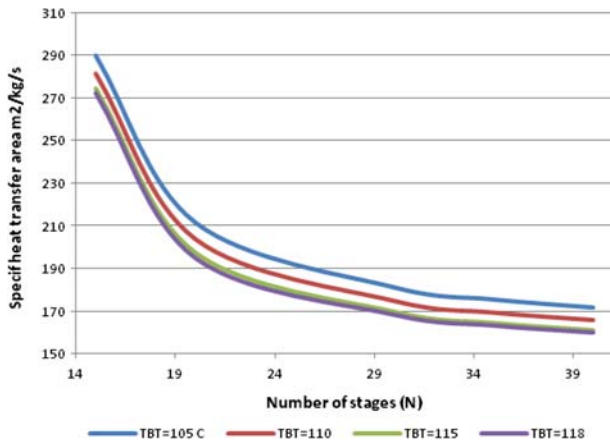


Fig. 6. Relation between specific heat transfer area and number of stages as a function of TBT.

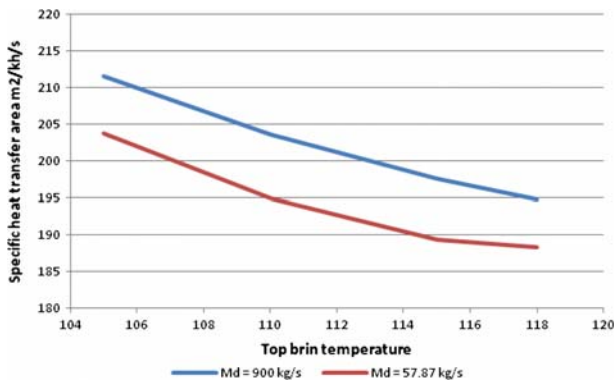


Fig. 7. Relation between specific heat transfer area and top brine temperature as a function of distillate product.

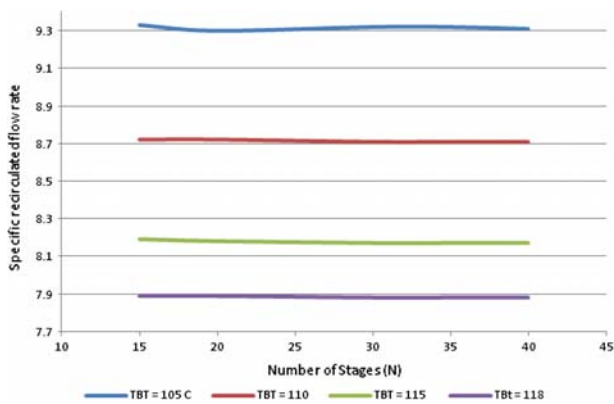


Fig. 8. Relation between specific recirculated flow and number of stages as a function of TBT.

increase which mean that there is an increase in the heat load of the plant at certain PR.

Fig. 8 represents the effect of the number of stages and top brine temperatures on the specific circulating

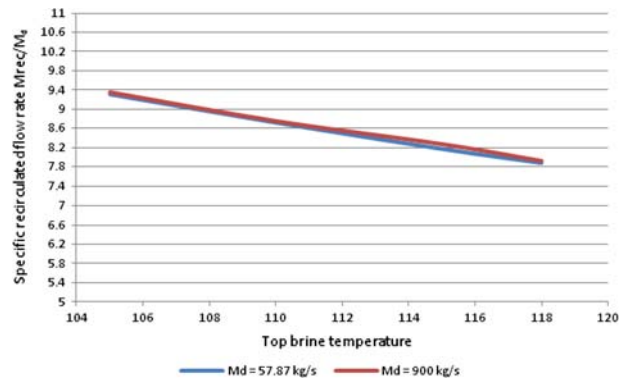


Fig. 9. Relation between specific recirculated flow rate and top brine temperature as a function of distillate product ($n = 20$).

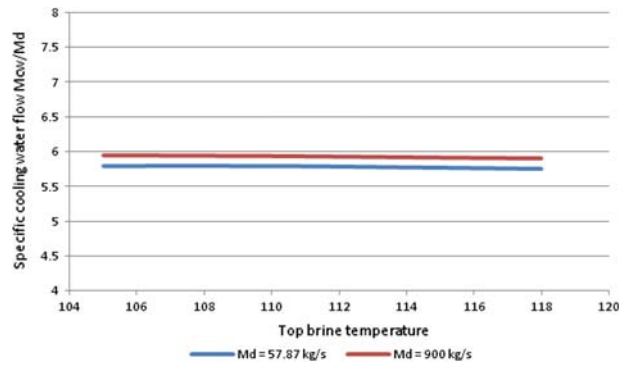


Fig. 10. Relation between specific cooling flow rate and top brine temperature as a function of distillate product ($n = 20$).

flow rate (sp. M_{rec}), it is clear that the circulating brine flow rate is completely independent of the number of stages and dependant on the top brine temperature. As the flashing range increases, the specific circulated brine decreases and consequently the pumping cost. Fig. 9 also illustrates the variation in the specific circulated flow rate as a function of the top brine temperature.

In Fig. 10, there is no change of the specific sea water cooling flow rate by change of the production capacity as the value of the PR kept constant, by this it is clear that the amount of the heat added to the system per unit production is constant, so the required cooling flow rate has no effect by increasing the production rate.

6. Model prediction data

A comparison of model data and field data is made for a number of actual plants; this is illustrated in Table 2 [7].

Table 2
Indicates the comparison between field and predicted data

| Plant | PR | Input design data | | | Calculated | Variables | |
|-------------------------------|-----|-------------------|----------|--|---|---------------------------|----------------------------|
| | | TBT (°C) | <i>n</i> | <i>M_d</i> (m ³ /d) | Sp. heat transfer area (m ² /kg/s) | Sp. <i>M_{cw}</i> | Sp. <i>M_{rec}</i> |
| (1) Shuweihat (Abu Dhabi UAE) | 9 | 111 | 21 | 75,670 | 222 | 5.3 | 8.5 |
| (2) Mirfa (Abu Dhabi UAE) | 8.9 | 110 | 21 | 34,000 | 227 | 5.3 | 8.7 |
| (3) Al Hidd (Bahrain) | 9 | 112 | 21 | 37,000 | 225 | 5 | 8.5 |
| (4) Jebel Ali "G" (Dubai UAE) | 8.8 | 115 | 21 | 34,080 | 212 | 5.3 | 8.2 |

The results shown in the above table are for medium and large capacities that varies from 34,000 to 76,000 m³/d; for the specific heat transfer area, it varies in the range of 200–250 m²/kg/s; the specific cooling flow rate varies in the range of 5–5.5 and the specific recirculated flow rate varies between 8 and 9. There is no actual data available for the specific heat transfer area; the specific cooling and recirculated flow rate. The calculated values are compatible with the field practice as, the specific value of the heat transfer area in the literatures vary between 200 and 300 m²/kg/s, and the values of the specific circulated flow rate vary in the range of 8–9. So the results show good agreement between predicted and field data.

7. Conclusions

Steady state analysis of Giant MSF recirculation brine is presented. This work describes the analysis of the MSF desalination plant, throughout this model results. This developed model is able to investigate the effect of some key parameters such as, top brine temperature, number of stages, recirculation flow rate, cooling flow rate that may affect on the performance of the MSF system during the steady state operation. The analysis output is the specific heat transfer area, specific brine recirculation, specific cooling flow rate. The model was validated by using previous studies and using actual data from existing plants. There is a good agreement between the predicted and real data. From this study, it can be concluded that:

- Through this study, both the specific heat transfer area and the weir load vary in the range of 175–300 m²/kg/s and 150–310 kg/s/m, respectively, also the stage width varies up to 25 m and the stage length varies in the range of 2–6 m.
- The specific recirculation flow rate varies in the range of 8–9.5 and the specific cooling flow rate varies in the range of 5–6.

- It is concluded that as the production capacities increases the specific heat transfer area increases also.
- It is concluded that there is no effect of the production increase on the specific cooling flow rate, and there is a slight change on the specific recirculated flow rate by change of the production rate although the PR is constant.
- It is clear that the system design is completely dependent on its productivity. The comparison between operating data of actual plants and the predicted data through this model shows adequacy agreement.

Appendix

Calculation of thermal and physical properties of water and water vapor [9]

- (1) The BPE depends on both the brine salinity *S* and the flashing temperature *T*. The BPE in °K is given by

$$BPE = S(B + CS)$$

Both coefficients *B* and *C* are functions of *T* as follows:

$$B = [6.71 + 6.43 \times 10^{-2}T + 9.74 \times 10^{-5}T^2]10^{-3}$$

$$C = [22.238 + 9.59 \times 10^{-3}T + 9.42 \times 10^{-5}T^2]10^{-5}$$

The salinity of brine flowing from the first chamber to the second one *S*₁ is related to the recirculated brine salinity *S*₀ by the following relationship:

$$S_1 \frac{M_{rec} \times S_0}{M_{rec} - D_1}$$

- (2) The following two correlations are used to calculate the non-equilibrium allowance

$$NEA_{10} = (0.9784)^{T_o} (15.7378)^H (1.3777)^{[w]10-6}$$

$$NEA = \left[\frac{NEA_{10}}{0.5DT_s + NEA_{10}} \right]^{0.3281L} [0.5DT_s + NEA_{10}]$$

The first equation is applicable only for stage of 10 ft in length, while the second one is used for stages of any other lengths.

- (3) The equation governing the temperature loss across the demister and condenser tubes

$$\Delta = \exp(1.885 - 0.02063 \times T_d) / 1.8$$

where, T_d is the temperature of the condensing vapor in °F and Δ are the losses

- (4) Vapor pressure of saturated water
 $P_v = 23.487 - 0.15T + 2.41 \times 10^{-4}T^2$
 where P_v = vapor pressure of saturated water, bar and T = saturated temperature, °K
- (5) Saturation temperature
 $T = 307.21 + 127.8P_v - 64.127P_v^2$
 where T = saturation temperature, °K and P_v = saturation vapor pressure, bar
- (6) Specific volume of water vapor
 $V_g = 1,248.643 - 1.91T + 3.651 \times 10^{-3}T^2$
 where V_g = specific volume of water vapor, m³/kg and T = temperature, °K
- (7) Specific volume of water
 $V_l = 5,611.453 - 46.436T + 0.1284T^2 - 1.185 \times 10^{-4}T^3$
 where V_l = specific volume of liquid, m³/kg and T = temperature, °K
- (8) Latent heat of evaporation
 $L_v = 2,589.583 + 0.9156T - 4.8343 \times 10^{-3}T^2$
 where L_v = latent heat of evaporation, kJ/kg
- (9) Dynamic viscosity of water
 $\mu = 1.278 \times 10^{-3} - 1.835 \times 10^{-5}T + 8.69 \times 10^{-8}T^3$
 where μ = water viscosity, kg/m s and T = temperature, °K
- (10) Specific heat of water at constant pressure
 $C_p = [A + BT + CT_2 + DT_3] \times 10^{-3}$
 where T = temperature, °C, S = water salinity, g/kg, $A = 4,206.8 - 6.6197S + 1.2288 \times 10^{-2}S^2$, $B = -1.1262 + 5.4178 \times 10^{-2}S - 2.2719 \times 10^{-4}S^2$, $C = 1.2026 \times 10^{-2} - 5.3566 \times 10^{-4}S + 1.8906 \times 10^{-6}S^2$, and $D = 6.87774 \times 10^{-7} + 1.517 \times 10^{-6}S^{-4} - 4.4268 \times 10^{-9}S^2$

Symbols

| | |
|-------|--|
| A | — heat transfer area, m ² |
| BBT | — bottom brine temperature, °C |
| BPE | — boiling point elevation, °C |
| C_p | — specific heat at constant pressure, kJ/kg K |
| d_i | — tube inner diameter, m |
| d_o | — tube outer diameter, m |
| g | — gravitational acceleration, m ² /s |
| h | — heat transfer coefficient, kW/m ² K |
| H | — enthalpy, kJ/kg |
| L | — latent heat, kJ/kg |
| LMTD | — logarithmic mean temperature difference, °C |
| M | — mass flow rate, kg/s |
| mgd | — millions gallons per day |
| N | — number of flashing chamber |
| NEA | — non-equilibrium allowance, °C |

| | |
|-------|--|
| Sumdt | — total temperature losses across stage, °C |
| T | — temperature, °C |
| TBT | — top brine temperature, °C |
| U | — heat transfer coefficient, kW/m ² K |
| V | — velocity, m/s |
| X | — salinity, ppm |

Greek

| | |
|----------|---------------------------------|
| Δ | — temperature difference, °C |
| ρ | — density, kg/m ³ |
| δ | — non-equilibrium allowance, °C |

Subscripts

| | |
|------|-----------------|
| b | — brine |
| bd | — blow-down |
| bh | — brine heater |
| cw | — cooling water |
| d | — distillate |
| dem | — demister |
| evap | — evaporator |
| f | — feed |
| i | — recovery |
| j | — rejection |
| sea | — seawater |
| v, s | — vapor |

References

- [1] N.H. Aly, A.K. El-Feky, Thermal performance of seawater desalination systems, *Desalination* 158 (2003) 127–142.
- [2] S.E. Aly, K. Fathalah, A mathematical model of a MSF system, *IDA World Congr.* 4 (1995) 203–226.
- [3] H.M. Ettouney, H.T. El-Dessouky, F. Al-Juwayhel, Performance of the once through multistage flash desalination, *Proc. Inst. Mech. Eng. Part A: Power Energy* 216 (2002) 229–242.
- [4] M.A. Darwish, Thermal analysis of multi stage flash desalination systems, *Desalination* 85 (1991) 59–79.
- [5] M.A. Soliman, A mathematical model for multi-stage flash desalination plants, *J. Eng. Sci.* 7 (1981) 2–10.
- [6] A. Husain, A. Woldai, A. Al-Radif, A. Kesou, R. Borsani, H. Sultan, P.B. Desphandey, Modeling and simulation of a multistage flash desalination plant, *Desalination* 97 (1994) 555.
- [7] M. Nabil, Abdel-Jabbar, Hazim Mohameed Qiblawey, Farouq S. Mjalli, Hisham Ettouney, Simulation of large capacity MSF brine circulation plants, *Desalination* 204 (2007) 501–514.
- [8] M.A. Darwish, M.M. El-Refae, M. Absel-Jawad, Developments in the multi-stage flash desalting system, *Desalination* 100 (1995) 35–64.
- [9] Hisham El-Dessouky, S. Bingulac, Solving equations simulating the steady state behavior of the multi-stage flash desalination process, *Desalination* 107 (1996) 171–193.
- [10] H. El-Dessouky, H. Ettouney, Study on water desalination technologies, Prepared for ESCAWA in January 2001.